Application of Continuous Vorticity Panels to General Unsteady Incompressible Two-Dimensional Lifting Flows

M. J. Kim* and D. T. Mook†
Virginia Polytechnic Institute and State University, Blacksburg, Virginia

Continuous vorticity panels are used to model general unsteady inviscid, incompressible, two-dimensional lifting flows. The geometry of the airfoil is approximated by a series of short straight segments having endpoints that lie on the actual surface. A piecewise linear, continuous distribution of vorticity over the approximated surface is used to generate the disturbance flow. The no-penetration condition is imposed at the midpoint of each segment and at discrete times. The wake is simulated by a system of discrete vortex cores (point vortices), which move at the local particle velocity. At each time step a new core is placed at the trailing edge, and the condition of constant circulation around wing and wake is imposed. Because the system is overdetermined, an optimization scheme is used to obtain simultaneously the unknown values of the surface velocity at the endpoints of the segments and the unknown value of the circulation around the core at the trailing edge. Comparisons are made with known exact solutions and wind tunnel data for one- and two-component airfoils in steady flow, and with other computed results and one experiment for unsteady flow. The present approach provides an attractive alternative to those developed earlier, being easy to formulate, easy to use, and very accurate.

Introduction

HERE we consider general unsteady, two-dimensional, incompressible, inviscid lifting flows. The present method is based on a piecewise linear, continuous distribution of vorticity over the surface. Such distributions of surface singularities have been used to model steady flows (see, for example, Raj and Gray[1]), but the extension to unsteady flows has not yet been effected. We describe one way this can be done.

A number of other papers have been devoted to unsteady, two-dimensional, lifting flows. Some are relevant to the present work and are mentioned at appropriate places throughout the present discussion. The present approach views the body as moving through the air and poses the mathematical problem in terms of a moving coordinate system attached to it. If the airfoil is deforming with time, then the moving coordinate system is attached to a reference configuration. The airfoil can execute arbitrary two-dimensional maneuvers.

The present approach provides an attractive alternative to the earlier treatments of this same problem; it is easy to formulate and to use, and it is very accurate. Its accuracy stems from the fact that the basic unknowns are primitive variables, the values of the potential-flow velocity on the surface of the airfoil.

Background

The position and orientation of the moving frame are given by $\boldsymbol{R}_A(t)$ and $\theta(t)$ as shown in Fig. 1. It follows that

$$\boldsymbol{R}=\boldsymbol{R}_A+\boldsymbol{r} \tag{1}$$

where $\boldsymbol{R}=X\boldsymbol{I}+Y\boldsymbol{J}$, $\boldsymbol{R}_A(t)=X_A(t)\boldsymbol{I}+Y_A(t)\boldsymbol{J}$, and $\boldsymbol{r}=x\boldsymbol{i}+y\boldsymbol{j}$.

Substantial differentiation of Eq. (1) yields

$$\boldsymbol{V}=\boldsymbol{V}_A+\boldsymbol{\Omega}\times\boldsymbol{r}+\boldsymbol{v} \tag{2}$$

where $\boldsymbol{V}$ is the velocity of a fluid particle with respect to the fixed reference frame (the absolute velocity), $\boldsymbol{v}$ the velocity with respect to the moving frame (the relative velocity), $\boldsymbol{V}_A$ the absolute velocity of the origin of the moving frame, $\boldsymbol{\Omega}$ the angular velocity of the moving frame ($\boldsymbol{\Omega}=\dot{\theta}\boldsymbol{k}$), and $\boldsymbol{r}$ the position of the fluid particle relative to the moving frame.

When the airfoil moves, it sets the air in motion and creates vorticity in the boundary layer on its surface. In an unsteady flow, the distribution of this vorticity changes, causing the circulation around the airoil to change. The Kelvin-Helmholtz theory and conventional wisdom dictate that the change in circulation around the airfoil is matched by a change in circulation around the wake of equal magnitude and opposite sign, that vorticity enters the wake when it is shed from the trailing edge, and that vorticity is convected away from the airfoil at the local particle velocity.

Using the ideas of boundary-layer theory, one can readily verify that the integral of curl $\boldsymbol{V}$ across the boundary layer equals the speed of the outer flow on the surface. The magnitude of the surface velocity is the unknown. Outside the boundary layer and wake the flow is irrotational. The loads

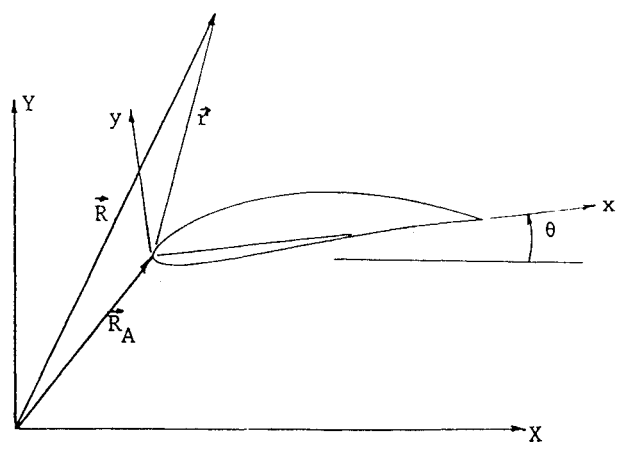

Fig. 1 Fixed and moving reference frames.

Received Jan. 8, 1985; presented as Paper 85-0282 at the AIAA 23rd Aerospace Sciences Meeting, Reno, NV, Jan. 14-17, 1985; revision received Jan. 27, 1986.

*Graduate Research Assistant, Engineering Science and Mechanics Department; presently Assistant Professor, Mechanical Engineering Department, Northern Illinois University, DeKalb, IL.

†Professor, Engineering Science and Mechanics Department. Member AIAA.

are computed from the pressure on the surface, which is given by Bernoulli's equation. The form of Bernoulli's equation applicable to a moving frame is discussed next.

The potential function expressed in terms of $\boldsymbol{R}$ and t is denoted by Φ, while the one in terms of $\boldsymbol{r}$ and t is denoted by ϕ. Both potentials describe the same velocity field; thus,

$$\boldsymbol{V} = \nabla_R \Phi = \nabla_r \phi \tag{3}$$

Because $\boldsymbol{r}$ must change with time when $\boldsymbol{R}$ is constant, the time derivatives are related by

$$\left.\frac{\partial \Phi}{\partial t}\right|_R = \left.\frac{\partial \Phi}{\partial t}\right|_r - \boldsymbol{V}\cdot(\boldsymbol{V}_A + \Omega \times \boldsymbol{r}) \tag{4}$$

where $/_R$ indicates $\boldsymbol{R}$ is constant and $/_r$ indicates $\boldsymbol{r}$ is constant. In a fixed reference frame Bernoulli's equation has the form

$$\left.\frac{\partial \Phi}{\partial t}\right|_R + \frac{V^2}{2} + \frac{P}{\rho} = H(t) \tag{5}$$

where V is the absolute speed, ρ the density, P the pressure, and $H(t)$ a spatially uniform function of time. At large distances from the airfoil and its wake, P is constant and V is zero. Hence we let $H(t) = P_\infty/\rho$ a constant. Using this and Eq. (4), one can rewrite Eq. (5) as

$$\frac{\partial \phi}{\partial t} - \boldsymbol{V}\cdot(\boldsymbol{V}_A + \Omega \times \boldsymbol{r}) + \frac{V^2}{2} + \frac{P}{\rho} = \frac{P\infty}{\rho} \tag{6}$$

It is convenient to introduce dimensionless variables (denoted by asterisks)

$$\boldsymbol{V} = U_c \boldsymbol{V}^*,\ \boldsymbol{V}_A = U_c \boldsymbol{V}_A^*,\ \Omega = \frac{U_c}{L_c}\Omega^* \tag{7a}$$

$$\boldsymbol{r} = L_c \boldsymbol{r}^*,\ t = \frac{L_c}{U_c} t^* \tag{7b}$$

where U_c and L_c are a characteristic speed and a characteristic length. (Here we take L_c to be the chord.) Substituting these definitions into Eq. (6) and then dropping the asterisks in the result leads to

$$C_p = \frac{P - P\infty}{\frac{1}{2}\rho U_c^2} = -2\frac{\partial \phi}{\partial t} + 2\boldsymbol{V}\cdot(\boldsymbol{V}_A + \Omega \times \boldsymbol{r}) - V^2 \tag{8}$$

Equation (8) is used to calculate the loads.

To obtain the surface velocity, one must impose the no-penetration boundary condition, a trailing-edge condition, and the requirement that the circulation around both airfoil and wake remain constant. These are discussed next.

For the moving airfoil the no-penetration boundary condition takes the form

$$(\boldsymbol{V} - \boldsymbol{V}_s)\cdot\boldsymbol{n} = 0 \tag{9}$$

everywhere on the surface of the airfoil, where $\boldsymbol{V}_s$ is the absolute velocity of a point in the surface of the airfoil, $\boldsymbol{V}$ the velocity the fluid particle in contact with that point, and $\boldsymbol{n}$ a vector normal to the surface at that point. If the airfoil is considered a rigid body, then $\boldsymbol{V}_s$ is given by an expression of the form

$$\boldsymbol{V}_s = \boldsymbol{V}_A + \Omega \times \boldsymbol{r}_s \tag{10}$$

where $\boldsymbol{r}_s$ is the relative position of the point in the surface. In general, the velocity of a fluid particle can be expressed as

$$\boldsymbol{V} = \boldsymbol{V}_B + \boldsymbol{V}_W \tag{11}$$

where $\boldsymbol{V}_B$ is the velocity induced by the vorticity on the surface and $\boldsymbol{V}_W$ the velocity induced by the vorticity in the wake. (For flows that appear steady in the moving frame, $\boldsymbol{V}_W = 0$.) Using Eqs. (10) and (11), one can rewrite Eq. (9) as

$$\boldsymbol{V}_B\cdot\boldsymbol{n} = (\boldsymbol{V}_A + \Omega \times \boldsymbol{r}_s - \boldsymbol{V}_W)\cdot\boldsymbol{n} \tag{12}$$

We require the pressures along the upper and lower surfaces to approach the same value at the trailing edge. This idea, of course, is common to all models of lifting flows. In establishing the statement of this requirement suitable for the present numerical scheme, we follow a procedure similar to the one developed by Basu and Hancock.[2] They referred to unpublished correspondence with E. C. Maskell, and they noted that Giesing[3] had earlier arrived at essentially the same conclusions. Recent experimental studies by Telionis and Poling[4] seem to support the conclusions. The ideas are discussed next.

In the potential-flow model of the trailing edge, we assume that the streamlines along the upper and lower surfaces, when viewed in the moving reference frame, always merge at the trialing edge where separation occurs. One must consider what is happening along each streamline. If the trailing edge is not a cusp, then the situation there can be described by one of the following:

1) Both merging streamlines have a sharp bend, and the streamline emanating from the trailing edge passes outside the wedge formed by the two tangents, as shown in Fig. 2a. If this happens, the speed along one of the merging streamlines (the bottom line in Fig. 2a) is infinite, while the speed along the other is zero at the trailing edge.

2) Only one merging streamline has a sharp bend; the other is smooth, and the streamline emanating from the trailing edge is tangent to one side of the wedge, as shown in Fig. 2b. If this happens, the speed is zero on the bent streamline and nonzero but finite on the other at the trailing edge.

3) Both merging streamlines have a sharp bend, and the streamline emanating from the trailing edge remains inside the wedge, as shown in Fig. 2c. If this happens, the speed is zero on both streamlines at the trailing edge.

To see the implications of these possibilities, we apply Bernoulli's equation at the trailing edge along the upper and lower surfaces. It follows from Eq. (8) that

$$C_{p\ell} - C_{pu} = 2\frac{\partial}{\partial t}(\phi_u - \phi_\ell) + V_u^2 - V_\ell^2 + 2(\boldsymbol{V}_\ell - \boldsymbol{V}_u)\cdot(\boldsymbol{V}_A + \Omega \times \boldsymbol{r}) \tag{13}$$

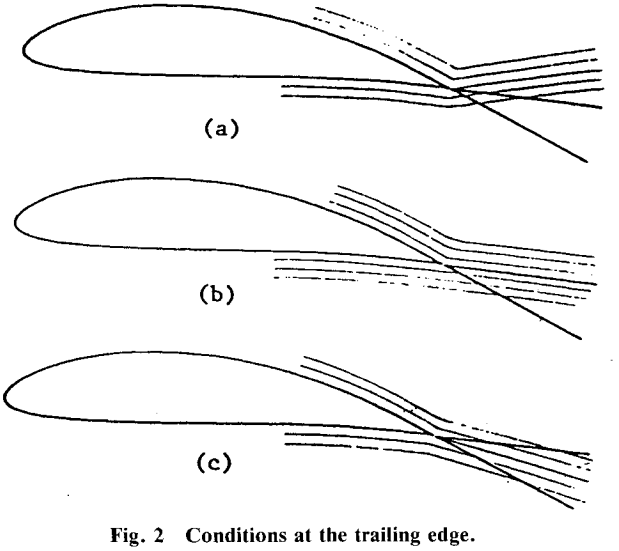

Fig. 2 Conditions at the trailing edge.

where the subscripts ℓ and u denote the values the different quantities approach along the lower and upper surfaces. The requirement that $C_{p\ell} = C_{pu}$ leads to

$$2\frac{d\Gamma}{dt} = V_\ell^2 - V_u^2 + 2(V_u - V_\ell)\cdot(V_A + \Omega \times r) \tag{14}$$

where Γ is the clockwise circulation around the airfoil.

For circulation around both airfoil and wake to remain constant, the rate of change of the circulation around the wake must be the negative of that given by Eq. (14).

Had the problem been posed in a fixed reference frame, Eq. (14) would have been replaced by

$$2\frac{d\Gamma}{dt} = V_\ell^2 - V_u^2 \tag{15}$$

One can use Eq. (2) to rewrite Eq. (14) in terms of the velocity relative to the moving frame v. The result is an equation having the form of Eq. (15), where the squares of the absolute velocity V_ℓ^2 and V_u^2 are replaced with their relative-velocity counterparts v_ℓ^2 and v_u^2. Equation (15) was given by Basu and Hancock as well as Telionis and Poling. Prandtl and Tietjens[5] gave the right-hand side of Eq. (15) as the expression for the addition of vorticity to the wake. Geising gave an equation valid for multi-energy flows that reduces to Eq. (15).

For case 1, $V_u = 0$ and $V_\ell = \infty$; hence, Eq. (14) suggests that the rate of production of circulation is infinite. For case 2, $V_u = 0$ and $V_\ell =$ a nonzero finite value; hence, Eq. (14) suggests that the rate of production of circulation is nonzero but finite. For case 3, $V_u = V_\ell = 0$; hence, Eq. (14) suggests that the rate of production of circulation is zero, with Γ constant.

The first case can be used to simulate the situation at the instant of an impulsive start. After the sudden start and while conditions are unsteady, the situation is modeled by the second case. The steady state is modeled by the third case.

There is no inconsistency with the speed on the upper-surface streamline differing from the speed on the lower-surface streamline at, and downstream of, the point of merger. This is the potential-flow imitation of the wake. There is no discontinuity in the pressure across the wake if the vorticity is convected at the local particle velocity (see, for example, Ref. 6, pp. 239-243).

In the case of a trailing-edge cusp, the streamlines have a sharp bend at the trailing edge when the rate of change of circulation is infinite and are otherwise tangent to the trailing-edge. When the rate of change of circulation is nonzero but finite, the speeds on the upper and lower surfaces approach different values. When the rate of change is zero, the speeds approach the same value.

Present Numerical Scheme

The surface of the airfoil is approximated by a series of short straight segments as shown in Fig. 3. The ends of the segments, which are called nodes, lie on the surface of the airfoil. The surface velocity is approximated by a continuous function that varies linearly between the nodes.

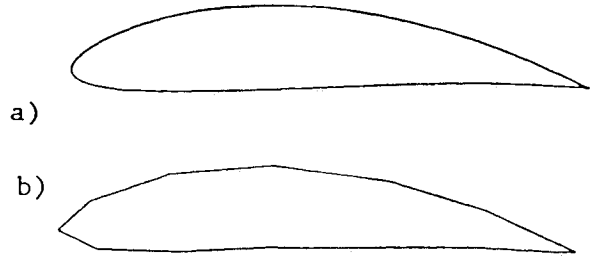

Fig. 3 Discretization: a) the actual airfoil profile; b) the airfoil after discretization.

For steady flows, it has been found that the use of a piecewise constant, discontinuous distribution of vorticity (or equivalently surface velocity) can lead to inaccuracies such as oscillating values of the vorticity on successive panels. Anderson[7] discussed some of these problems. The same problems occur in unsteady flows. The use of a linearly varying, continuous distribution of vorticity eliminates these problems.

The main building blocks of the present method are the formulas for the velocity fields induced by a linearly varying vortex sheet and a point vortex core (point vortex). Referring to Fig. 4, we can write the velocity components at a point (x,y) as follows:

$$\text{Case 1: } v_x = (1-\tilde{x})\Delta\theta - \tilde{y}\ell n(R) \tag{16a}$$

$$v_y = (1-\tilde{x})\ell n(R) + \tilde{y}\Delta\theta - 1 \tag{16b}$$

$$\text{Case 2: } v_x = \tilde{y}\ell n(R) + \tilde{x}\Delta\theta \tag{17a}$$

$$v_y = 1 + \tilde{x}\ell n(R) - \tilde{y}\Delta\theta \tag{17b}$$

In Eqs. (16) and (17)

$$\tilde{x} = \frac{x}{\ell},\quad \tilde{y} = \frac{y}{\ell} \tag{18a}$$

$$\Delta\theta = \theta_2 - \theta_1 = \tan^{-1}[(1-\tilde{x})/\tilde{y}\,] - \tan^{-1}(-\tilde{x}/\tilde{y}) \tag{18b}$$

and

$$R = \frac{R_2}{R_1} = \left[\frac{(1-\tilde{x})^2 + \tilde{y}^2}{\tilde{x}^2 + \tilde{y}^2}\right]^{1/2} \tag{18c}$$

For the vortex core having clockwise circulation 2π, the velocity field is

$$v_x = y/(x^2+y^2),\ v_y = -x/(x^2+y^2) \tag{19}$$

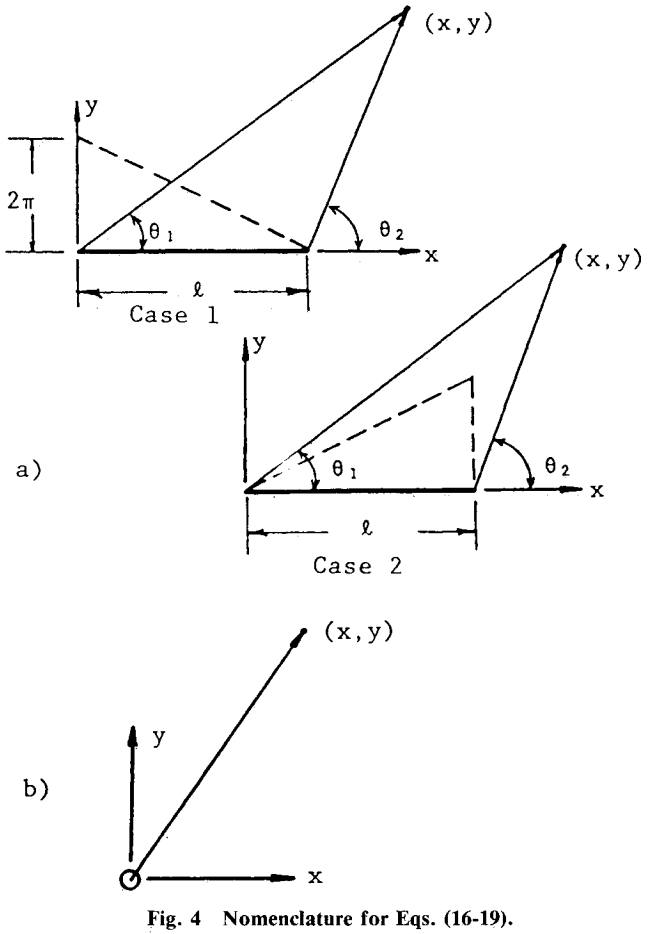

Fig. 4 Nomenclature for Eqs. (16-19).

Next the procedure for general unsteady flows is described. It follows from Eq. (14) and the requirement of constant circulation around airfoil and wake that, during a small time interval Δt, a vortex having approximately the circulation

$$\Delta\Gamma_w = -\tfrac{1}{2}[V_\ell^2 - V_u^2 + 2(V_u - V_\ell)\cdot(V_A + \Omega\times r)]\Delta t \quad (20)$$

is added to the wake. With the present method this vortex is modeled as a discrete point, or core. One is formed at each time step. These cores are convected away from the trailing edge at the local particle velocity and constitute the wake. Instead of using Eq. (20) directly, the present method approximates conditions at the trailing edge by setting both v_u and v_ℓ equal to zero and placing a core of unknown strength there.

The zero values of v_u and v_ℓ are consistent with the requirement for steady flow around airfoils of nonzero trailing-edge angle. As the numerical examples in the next section show, this is also the proper choice for airfoils with a trailing-edge cusp. For unsteady flows, either v_ℓ or v_u is zero; in general, both are not zero simultaneously. The contribution to the velocity field induced by this nonzero element is approximated by the contribution induced by the discrete core placed at the trailing edge. The two contributions are nearly the same. Closely spaced, discrete cores are then used to simulate the wake. Numerical examples show that the procedure is robust, showing good convergence characteristics. Further discussion of this approximation can be found in Ref. 3.

In a recent study, Duffy, et al.,[8] who considered a sinusoidally oscillating flat plate, arrived at a result equivalent to Eq. (20). They used a finite-element representation of the plate, which is essentially a two-dimensional version of the vortex-lattice method. They represented the wake with discrete vortex cores, as we do, but they did not convect these cores at the local particle velocity. Instead, they moved the cores at the velocity of the undisturbed freestream. As a result, their wakes are always flat and parallel to the freestream.

The no-penetration boundary condition, Eq. (12), is only imposed at discrete times and discrete points. There is one point in each element, called the control point, where this condition is enforced. It lies on the straight segment midway between the nodes. The normal to the surface is approximated by the perpendicular to the straight segment.

Using Eqs. (16-19), one can develop an influence matrix and replace Eq. (12) with the following:

$$\sum_{j=1}^{N} A_{ij}\gamma_j + T_i\Gamma_{TE} = (V_A + \Omega\times r_i - V_{Wi})\cdot n_i \quad (21)$$

for $i = 1,2,\ldots, N-1$. There are N modes and $N-1$ segments. Here A_{ij} is the normal component of the velocity at the control point of element i induced by unit surface speed at node j, and γ_j is the unknown value of surface speed at node j. T_i is the normal component of velocity induced by a discrete vortex core of unit circulation at the trailing edge, and Γ_{TE} is the unknown circulation around the core at the trailing edge. V_{Wi} is the velocity induced by all the cores in the wake except the one at the trailing edge. n_i is the unit vector perpendicular to the surface of element i.

In addition to Eq. (21), there is the condition at the trailing edge

$$\gamma_1(\text{or } V_\ell) = \gamma_N(\text{or } V_u) = 0 \quad (22)$$

and the condition of constant circulation around airfoil and wake

$$\int_c \nabla\cdot dr + \sum_{i=1}^{M}\Gamma_i = 0 \quad (23)$$

where C is a path around the airfoil through the trailing edge and the Γ_i are the circulations around the M cores making up the wake where $\Gamma_M = \Gamma_{TE}$. The integral is evaluated explicitly on the basis of a linear distribution of vorticity (or speed).

Equations (21-23) form a system $N+2$ equations for $N+1$ unknowns (the γ_i and Γ_{TE}). Hence we obtain the unknowns by an optimization technique. Specifically, we minimize the sum of the squares of the errors of Eq. (21) subject to the two equality constraints given by Eqs. (22) and (23).

After the unknowns have been obtained, the wake is convected. Then the unknowns are obtained again. This procedure can be repeated indefinitely. All one needs to start the procedure is a set of initial conditions (i.e., positions and circulations for the cores in the wake).

To convect all the cores in the wake, we use

$$r(t+\Delta t) = r(t) + V[r(t)]\Delta t \quad (24)$$

In earlier treatments, Giesing[9] and Basu and Hancock[2] also approximated the airfoil by a series of short straight segments. In contrast with the present method, they used a piecewise constant, discontinuous distribution of sources. In addition, they distributed a layer of constant-strength vorticity over the surface of the elements. The vorticity was used to satisfy the trailing-edge condition. Instead of solving for the surface velocity at the nodes, as one does with the present method, they solved for the strengths of the sources and vorticity. Then they calculated the surface velocity at the control points. Giesing also modeled the wake with cores convected at the local particle velocity, while Basu and Hancock used one element of distributed vorticity and used cores from then on.

Giesing used a prediction-correction scheme to convect the cores in the wake, a scheme that doubles the number of times the velocity is calculated in the wake. For the small step sizes used here, we found very little difference between the results obtained by the two procedures. All the results presented here are based on Eq. (24).

Equations (19) are used to calculate the velocity field generated by the wake. These expressions have an algebraic singularity; hence, following the usual practice, we introduce a cutoff length. Whenever the distance between the field point and the core is less than the cutoff length, the contribution of that core is ignored. For all the present calculations the cutoff length is the chord divided by twice the number of elements. Numerical experimentation has shown that the results depend on the cutoff length, but there is a range for which the results are very nearly constant. The present choice lies in this range.

Numerical Examples

A. Steady Flows

The dual purpose of considering steady flows is to establish the trailing-edge condition for both cusp and nonzero wedge angle and to demonstrate the accuracy of the present scheme. For steady flow, $V_W = 0$, $\Omega = 0$, and $V_A = u$, a unit vector of constant direction.

We consider von Kármán-Trefftz airfoils defined by

$$z = z_T\frac{(\zeta+\zeta_T)^n + (\zeta-\zeta_T)^n}{(\zeta+\zeta_T)^n - (\zeta-\zeta_T)^n} \quad (25)$$

Equation (25) transforms the unit circle in the ζ plane into the airfoil in the z plane. z_T is the point at the trailing edge of the airfoil and ζ_T is its image. Some discussion of these airfoils can be found in Karamcheti.[6] The trailing-edge wedge angle (see Fig. 2) is related to the exponent n according to

$$\beta(2-n)\pi \quad (26)$$

The special case of $n = 2$ yields a Joukowski airfoil, which has a cusp trailing edge.

For steady flows, Eq. (21) is modified by setting Γ_{TE} and V_{Wi} equal to zero, and Eq. (23) is dropped. We consider two possibilities for the condition at the trailing edge: 1) γ_1 (or

v_ℓ) + γ_N(or v_u) = 0 and 2) Eq. (22). Either possibility is the equivalent of the so-called Kutta condition and leads to a unique value of the circulation around the airfoil. For the former, we can eliminate one unknown and use Eq. (21) directly; the number of unknowns is the same as the number of equations. For the latter, we can eliminate two unknowns; the number of equations is one more than the number of unknowns, and we use an optimization scheme (specifically, we make the sum of the squares of the normal components of the relative velocity at the control points a minimum).

Raj and Gray also set $v_\ell = v_u = 0$, but then, instead of using an optimization scheme, they simply ignored one of the control points. Such a scheme is also described by Anderson.[7] This scheme raises the question of which control point to ignore. The results can vary considerably, depending on the choice. The present scheme eliminates the need to make such a choice, though one can arbitrarily weight the squares of the normal components at the control points and hence introduce some arbitrariness. In all the present results, the weighting is uniform.

The results for the first way of treating the trailing edge ($v_\ell + v_u = 0$) are given in Tables 1 and 2. In Table 1 the value of n in Eq. (27) is 1.95. For a small number of elements, the results are encouraging. But clearly the trend is wrong as the number of elements increases; v_u and v_ℓ change sign and are inconsistent with physical demands. The situation is worse when $n = 2$, as the results in Table 2 show. For a noncusp trailing edge, the values of v_u and v_ℓ should approach zero. For a cusp these values are not expected to approach zero, but here the signs of v_u and v_ℓ are inconsistent with the requirement of smooth flow from the trailing edge and there is no indication of convergence.

The problem stems from the fact that the elements near the trailing edge become more nearly coincident as the number of elements increase, and the results become vulnerable to round-off error. As a consequence, the trailing edge is better modeled as a single element that merges the vortex sheets on the upper and lower surfaces and has zero combined vorticity at the trailing edge. Without any modifications to accommodate the cusp and without experiencing any numerical problems, the second way of treating the trailing edge, which sets $v_u = v_\ell = 0$ and uses optimization, can in effect accomplish the merger.

The lift is accurately predicted by both methods (but the lifts predicted by the two are not quite the same) because the effect of the irregularity at the trailing edge cancels. Using a total of only eight elements to model both the upper and lower surfaces, the present procedure predicts the lift to within 5%.

As a second example, we consider a NACA 23012 airfoil at various angles of attack. The experimental pressure measurements of Wenzinger[10] are compared with the predictions of the present method in Fig. 5. The agreement is generally quite good; however, in part e of Fig. 5, the measurements suggest the presence of a separation bubble, which is not modeled by the present approach. In Fig. 6 experimental and numerical results are shown for the same airfoil in the presence of an external airfoil flap. Here Eq. (22) is imposed at both trailing edges. There is interaction between the two airfoils. The no-penetration condition on each airfoil simultaneously accounts for the disturbances created by both. Again the agreement is quite good. This suggests that the present method correctly captures the aerodynamic interference.

Table 1 Surface velocity at trailing edge, $n = 1.95$

NEM	Top	Bottom
20	+0.02954	−0.02954
40	−0.27155	0.27155
80	−0.52643	0.52643
160	−0.59926	0.59926

Table 2 Surface velocity at trailing edge, $n = 2$ (cusp trailing edge)

NEM	Top	Bottom
20	−2.78794	2.78794
40	−20.55102	20.55102
80	−122.39677	122.39677
160	−488.51154	488.51154

B. Unsteady Flows

In the first example, a symmetric von Kármán-Trefftz airfoil is advancing at a constant speed while executing a sinusoidal heaving motion. The angle θ (Fig. 1) is always zero

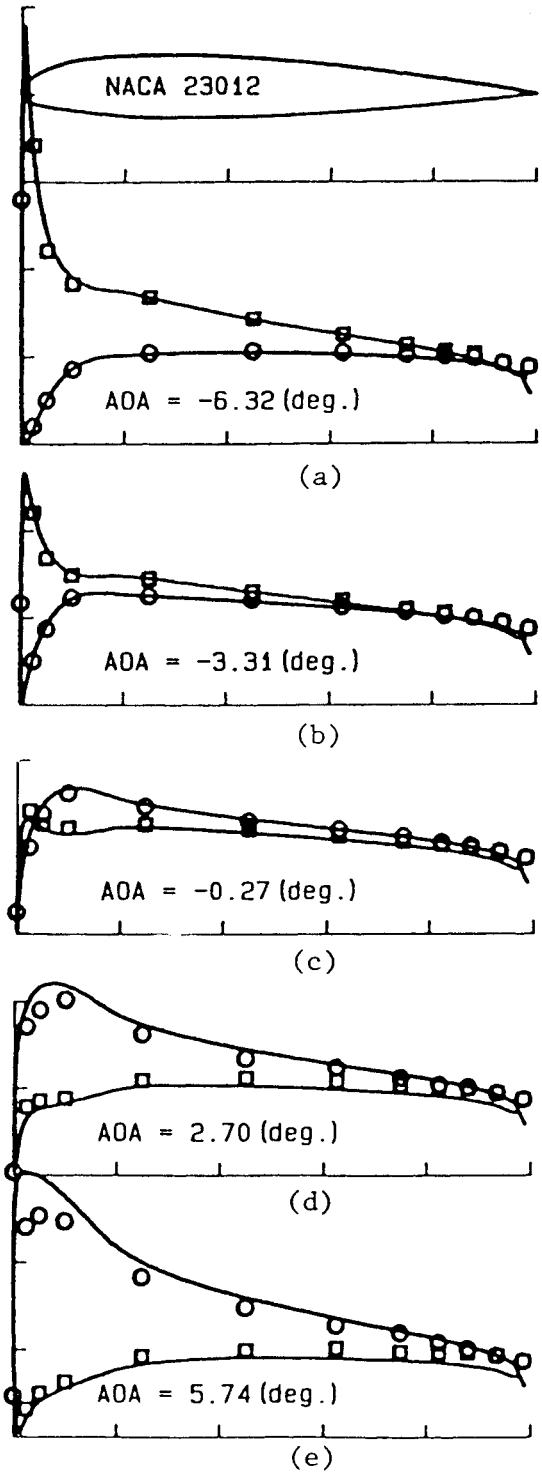

Fig. 5 Comparison of the predicted pressure distribution (□) with the experimental data of Wenzinger[10] (o,) for a NACA 23012 airfoil at various angles of attack (AOA).

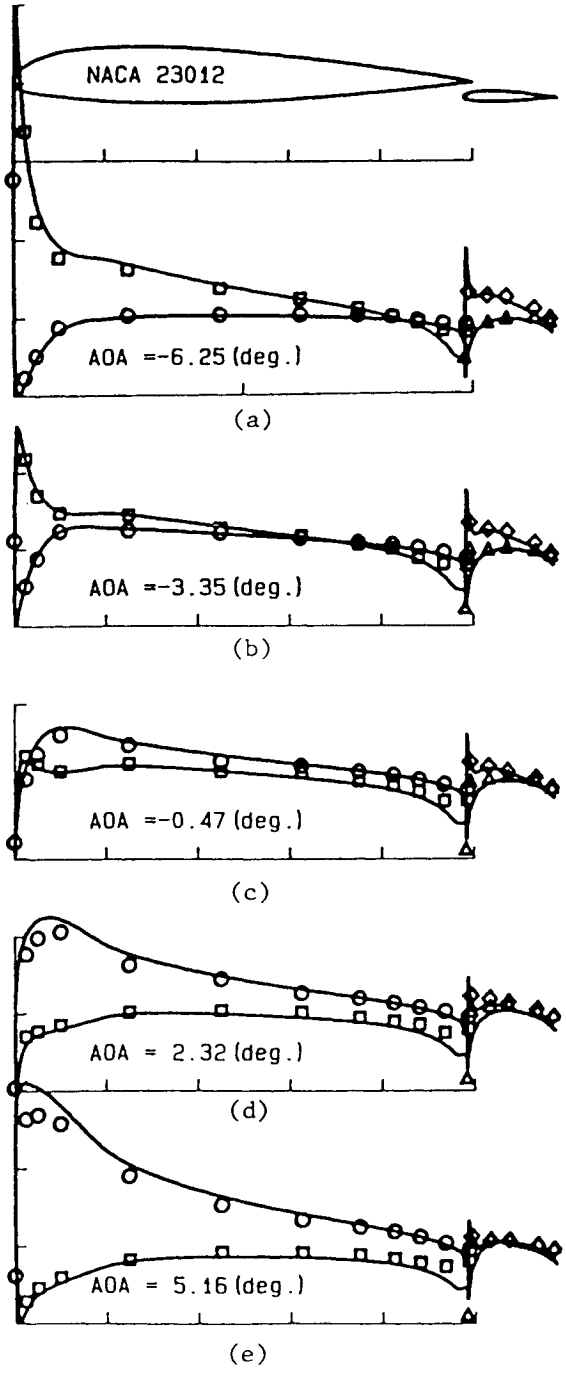

Fig. 6 Comparison of the predicted pressure distribution (□) with the experimental data of Wenzinger[16] (o,) for a NACA 23012 airfoil and flap at various angles of attack (AOA).

and

$$Y_A(t) = 0.018\sin\omega t$$

These conditions imitate the experiment of Bratt.[11] For Fig. 7, $\omega = 4.3$, which is the smaller of the two reduced frequencies considered by Bratt. In Figs. 7a, 7b, and 7c, 20, 40, and 80 elements, respectively, are used. As the number of elements increases, the time step correspondingly decreases and the cores in the wake become more densely packed. The time step is chosen to be approximately the length of time required for a fluid particle, moving at the characteristic speed, to travel the length of the element on the lower surface at the trailing edge. There appears to be convergence. In Fig. 7c, the discrete cores in the wake are so densely packed that near the trailing edge the graphical representation resembles a continuous line.

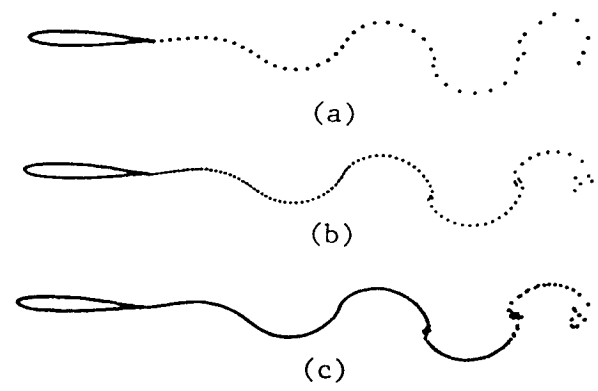

Fig. 7 Positions of vortex cores in the wake behind a sinusoidally ($\omega = 4.3$) heaving airfoil: a) 20 elements, b) 40 elements, and c) 80 elements.

Fig. 8 Positions of vortex cores in the wake behind a sinusoidally ($\omega = 17$) heaving airfoil.

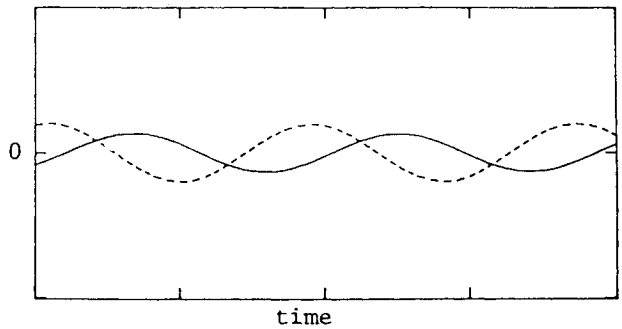

Fig. 9a --- position and ——— circulation for the sinusoidally ($\omega = 4.3$) heaving airfoil as functions of time.

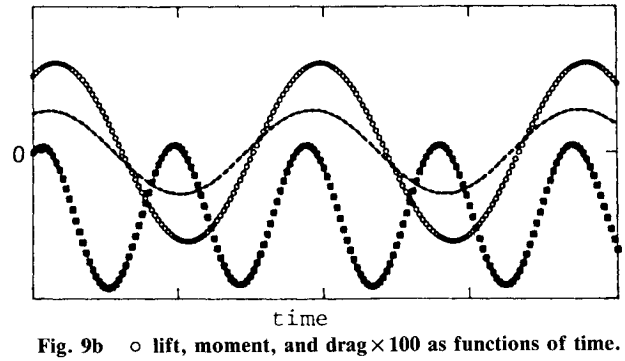

Fig. 9b o lift, moment, and drag × 100 as functions of time.

Similar results are shown in Fig. 8 for $\omega = 17$, the larger of the two frequencies considered in the experiment. The results in both figures are in good qualitative agreement with the smoke visualization[11] of the flow, the numerical results obtained earlier by Giesing,[9] and the semianalytical results of Katz and Weihs[12] for a flat plate.

Attempts to model the wake with continuous elements of vorticity were generally unsuccessful and certainly not robust, as the present approach is. Figures 7 and 8 clearly show the problem: Continuous elements are not able to produce the clustering shown in these figures. From the experiment it appears that vorticity does concentrate, and hence this clustering of discrete vortex cores is likely to be an accurate imitation of the actual flow.

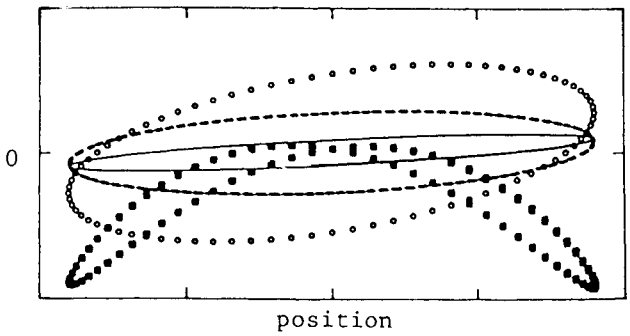

Fig. 10 o lift, --- moment, drag × 100, and ——— circulation as functions of position for the sinusoidally ($\omega = 4.3$) heaving airfoil.

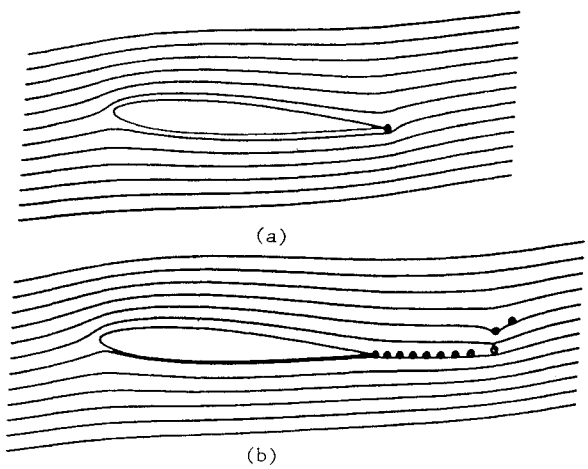

Fig. 11 Streamlines and positions of cores in the wake for an impulsively started airfoil: a) just after the start and b) after several time steps.

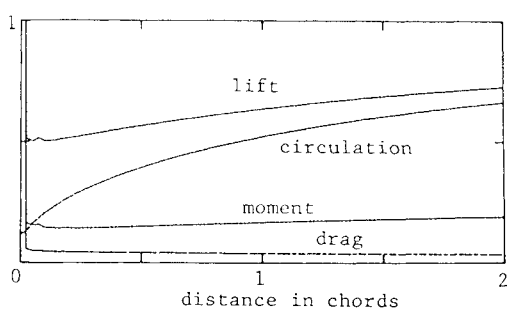

Fig. 12 Lift, circulation, moment, and drag × 100 as a function of distance traveled for an impulsively started airfoil.

There are many closely packed cores in the wake so that the velocity field they generate is quite smooth very near the wake. Consequently, the predicted effect of the wake on the wing is most probably accurate. One would expect the accuracy to be poorest near the trailing edge.

In Fig. 9 the lift, moment, drag, circulation, and position are shown as functions of time for the lower of the two frequencies. These results show that the loads are not in phase with each other or the motion. It is interesting to see that the mean value of the drag is negative, indicating that the pumping action of the airfoil produces a small thrust. The loads and circulation converge rapidly as the number of elements increase.[13] In Fig. 10, lift, moment, drag, and circulation are plotted as functions of position in the y direction for the same frequency. Hysteresis is clearly evident.

The time-dependent loads are obtained by integrating the pressure over the surface. The velocity potential ϕ is obtained by numerically evaluating a line integral. Several different

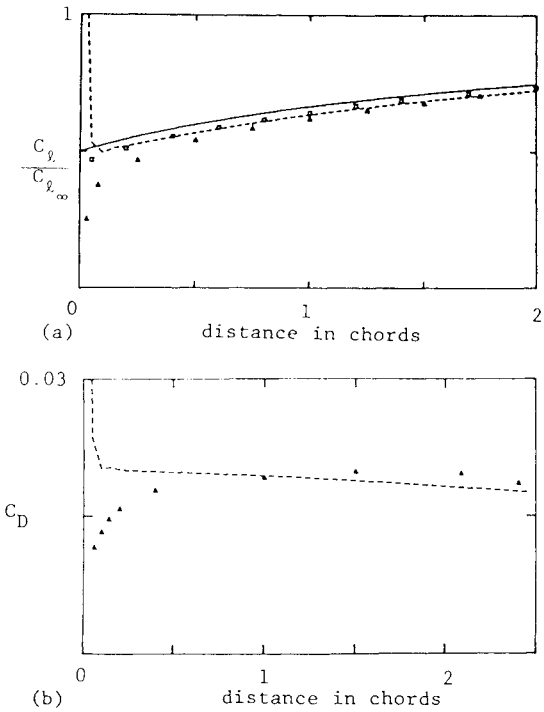

Fig. 13 Lift (a) and drag (b) as functions of distance traveled for an impulsively started airfoil — — — Wagner,[15] and Giesing,[9,17] Δ Basu and Hancock,[2] and - - - present results.

paths from the same starting point and several different starting points were used to check the results. A finite-difference formula is used to obtain the derivative of ϕ with respect to time. Giesing[9] evaluated ϕ analytically.

In the second example, a symmetric von Kármán-Trefftz airfoil is impulsively started and then moved forward at constant velocity and fixed angle θ (Fig. 1). In Fig. 11 the streamlines and positions of cores in the wake are shown. In Fig. 11a, the motion has just started, and the wake consists of only one vortex core at the trailing edge. The situation after many time steps is shown in Fig. 11b. The results in Fig. 11 closely resemble the figures in the texts by Karamcheti (Ref. 6, p. 394) and Prandtl and Tietjens.[5] Further numerical experiments[13] showed that the results converged rapidly as the number of elements increased.

In Fig. 12, the lift, moment, drag, and circulation are shown as functions of the distance traveled. The zero position corresponds to the instant the first core forms at the trailing edge; hence circulation is not zero there. It is interesting to note the large initial values of the loads. The small wiggles near the position where minimum lift occurs are probably a numerical aberration caused by the use of discrete cores. The drag decreases monotonically, but the lift and pitching moment about the nose of the airfoil first decrease rapidly and then grow slowly. The minimum value of lift and moment occur when the airfoil has traveled approximately one-tenth chord. Graham[14] and Giesing[17] predicted similar behavior for the lift. The present results for lift are compared with those of Basu and Hancock,[2] Giesing,[9] and Wagner[15] in Fig. 13a. Shortly after the start, all are in close agreement in spite of the fact that Wagner's results are for a flat plate and the others are for thick airfoils. In Fig. 13b, the present results for drag are compared with those of Basu and Hancock. The reason for the difference is not known.

In Fig. 14, the present results are compared with the experimental data of Walker (which can be found in the text by Goldstein[16]) and the analytical results of Wagner for a flat plate. In the experiment, a symmetric Royal Air Force (R.A.F.) 30 airfoil was placed in a long towing tank. The airfoil was started suddenly in an attempt to create an impulsive start and then moved at constant speed. The angle of attack was 7.5 deg. Oil drops suspended in the water and illuminated by a

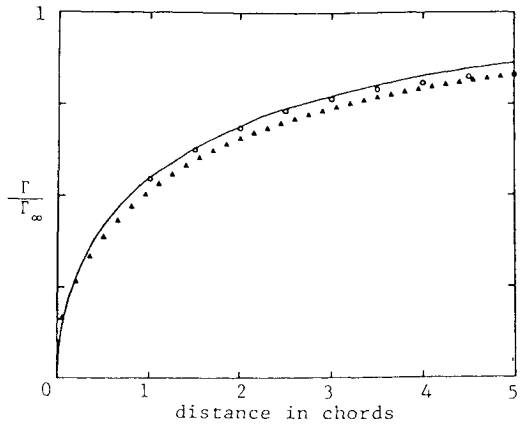

Fig. 14 Circulation as a function of distance traveled for impulsively started airfoils. — — — Wagner,[15] o Walker (see Goldstein[16]), and Δ present results.

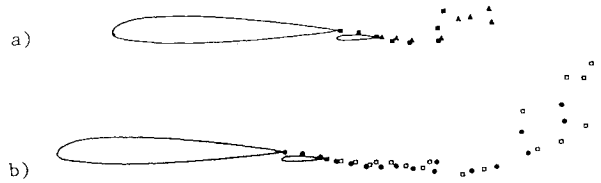

Fig. 15 Positions of vortex cores in the wakes behind an impulsively started airfoil and flap: a) after several time steps and b) after many time steps.

bright light were photographed. Exposures of known short duration yielded the velocity field. The circulation was obtained by evaluation of a line integral around the airfoil. The present results are for a symmetric von Kármán-Trefftz airfoil having the same thickness as the R.A.F. 30.

The final example is an impulsively started airfoil with flap. These are the same airfoil and flap used in the example of steady flow. For the purpose of illustrating the nature of this problem, we suppose that the number of nodes on the main airfoil is the same as that on the flaps—N nodes and $N-1$ elements. Equation (21) forms a system of $2N-2$ equations; the trailing-edge constraints, Eq. (22), yield four additional equations; and the requirement that the circulations around both airfoils and their wakes remain constant gives two more. There is a total of $2N+4$ equations and $2N+2$ unknowns (the γ_i on both and Γ_{TE} for both). Again the optimization scheme is used, the trailing-edge condition and the requirement of constant circulation being treated as constraints.

Figure 15 shows the development of the wake with time. The vorticity from the main airfoil is drawn down very near the surface of the flap, and the two wakes appear to merge at the trailing edge of the flap. In Fig. 16, the computed streamlines are shown at the instant the first cores form at the trailing edges and in the steady state. Figure 16b corresponds to the numerical data in Fig. 6.

Applications of the present method for other cases not shown here can be found in the thesis by Kim.[13]

Conclusions

A method for modeling general unsteady two-dimensional lifting flows is developed. The problem is posed in terms of a coordinate system fixed to a reference configuration of the moving airfoil. A vortex sheet is wrapped around the surface of the airfoil. The vorticity (or equivalently the surface velocity) is a continuous, linear function of position of the airfoil. As an imitation of conditions at the trailing edge, the surface velocity there is replaced by a discrete vortex core. During each time step, this core is shed into the wake from the trailing edge and a new core is formed. The cores that have been shed model the wake. Each is convected at the local particle velocity.

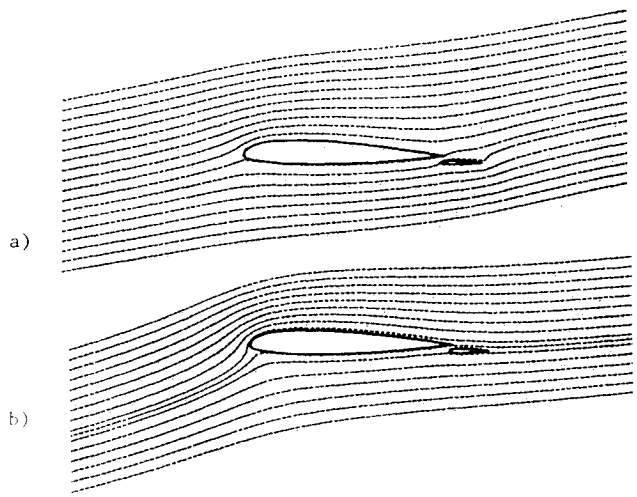

Fig. 16 Streamlines around an impulsively started airfoil and flap: a) just after the start and b) steady state.

At each time step, the unknowns are the values of the surface velocity at discrete points around the airfoil and circulation around the new core at the trailing edge. Because the system is overdetermined, these are obtained by an optimization scheme.

The present predictions are in good agreement with experimental data and other computations.

As an alternative to methods developed earlier, the present approach is easy to formulate, easy to use, and very accurate.

References

[1]Raj, P. and Gray, R. B., "Computation of Two-dimensional Potential Flow Using Elementary Vortex Distributions," *Journal of Aircraft*, Vol. 15, Oct. 1978, pp. 698-700.

[2]Basu, B. C. and Hancock, G. J., "The Unsteady Motion of a Two Dimensional Airfoil in Incompressible Inviscid Flow," *Journal of Fluid Mechanics,* Vol. 87, July 1978, pp. 159-168.

[3]Giesing, J. P., "Vorticity and Kutta Condition for Unsteady Multi-Energy Flows," *Journal of Applied Mechanics*, Vol. 36, Series E, March, 1969, pp. 608-613.

[4]Telionis, D. P. and Poling, D. R., "The Response of Airfoils to Periodic Disturbances—The Unsteady Kutta Condition," AIAA Paper 84-0050, 1984.

[5]Prandtl, L. and Tietjens, O. G., *Fundmentals of Hydro and Aeromechanics*, Dover Publications, Inc., New York, 1957, Chap. 12.

[6]Karamcheti, K., *Principles of Ideal-Fluid Aerodynamics*, John Wiley & Sons, New York, 1966, pp. 239-243, 394, and 448-489.

[7]Anderson, J. D., *Fundamentals of Aerodynamics*, McGraw-Hill Book Co., New York, 1984, Chap. 4.

[8]Duffy, R. E., Czajkowski, E., and Jaran, C., "Finite Element Approximation to Theodorsen's Solution for Non-steady Aerodynamics of an Airfoil Section," AIAA Paper 84-1540, 1984.

[9]Giesing, J. P., "Nonlinear Two-dimensional Unsteady Potential Flow with Lift," *Journal of Aircraft,* Vol. 5, March 1968, p. 135-143.

[10]Wenzinger, C. J., "Pressure Distribution over an NACA 23012 Airfoil with an NACA 23012 External Airfoil Flap," NACA Rept. 614, July 1937.

[11]Bratt, J. B., "Flow Patterns in the Wake of an Oscillating Airfoil," Royal Aeronautical Establishment, R&M 2773, 1953.

[12]Katz, J. and Weihs, D., "Behavior of Vortex Wakes from Oscillating Airfoils," *Journal of Aircraft*, Vol. 15, Dec. 1978, pp. 861-863.

[13]Kim, M. J., "Applications of Panel Methods for Subsonic Aerodynamics," Ph.D. Thesis, Virginia Polytechnic Institute and State University, Blacksburg, VA, Jan. 1985, Chap. 3.

[14]Graham, J. M. R., "The Lift on an Aerofoil in Starting Flow," *Journal of Fluid Mechanics*, Vol. 133, Aug. 1983, pp. 413-425.

[15]Wagner, H., "Uber die Entstehen dynamischer Auftriebs von Traglugeln," *ZAMM—Zeitschrift fur angewandte Mathematike und Mechanik*, Vol. 5, 1925, pp. 17-35.

[16]Goldstein, S., *Modern Developments in Fluid Dynamics*, Vol. 2, Dover Publishing Co., New York, 1965, p. 460-461.

[17]Giesing, J. P., "Nonlinear Interaction of Two Lifting Bodies in Arbitrary Unsteady Motion," *Transactions of ASME*, Vol. 90, Series D, Sept. 1968, pp. 387-394.